Geo-Resilience 2023 Conference, Cardiff, Wales
D.G. Toll & M.G. Winter (Eds)
British Geotechnical Association, London. 2024
https://doi.org/10.53243/Geo-Resilience-2023-7-6

Perspectives on Practical Tools, Best Practice and Emerging Technologies in the Application of Geophysics for Enhancing Resilience to Geohazards

Jim WHITELEY[1], Edward COX[2], Ady KOE[1]

[1]Atkins, The Hub, Bristol, United Kingdom
[2]Atkins, Nova North, London, United Kingdom
Corresponding author: Jim Whiteley (jim.whiteley@atkinsglobal.com)

Abstract

Geophysical methods contribute to improved georesilience by providing high-resolution and multi-dimensional subsurface information using non-invasive approaches. Emulating these attributes over the same spatial extent using intrusive methods can be expensive, time consuming and carries a higher carbon footprint. The use of geophysics in ground engineering is well established, particularly as part of ground investigation. However, recent technological developments in the field stand to deepen the integration of geophysics and intrusive investigation to improve georesilience, particularly in the context of geohazards. These technological developments include: i) the maturation of 3D geophysical imaging techniques to solve 3D geotechnical problems, ii) better integration of data using multi-method geophysical surveys and / or field-estimated or laboratory-measured geotechnical properties, and iii) improved data inversion, integration, interpretation and visualisation using open-source, community-supported software packages.

In this paper, we aim to contextualise these technical developments within the cultural change that is taking place across the ground engineering community with regards to how we gather, manipulate and present geohazards data. This change has seen an increasing recognition for the need to investigate, model and interpret ground conditions using multi-dimensional, high-resolution, digital data. We present an example of a 3D electrical resistivity tomography survey to characterise potential karst features, and the role this data plays in increasing georesilience by contributing high-resolution, spatially continuous data to improve our understanding of geohazards.

Keywords: Geophysics, geohazards, ground engineering, 3D

1. Introduction: engineering geophysics in the digital era

There has been a paradigm shift in the use of digital geoscientific data in ground investigation in the last 50 years. Discussion around the relative importance and systemic benefits and challenges posed by new technologies is active (e.g., Griffiths, 2019, Hearn, 2019). However, recent innovations in cost-effective and user-friendly digital technologies, coupled with dramatic increases in computing power and affordability, have permanently changed the way that geoscientific data are acquired, analysed, stored and shared for the purposes of ground engineering (McCaffrey et al., 2005). As geoscientific datasets increase in coverage, resolution, accuracy and diversity of application, new analytical solutions are being sought from the fields of data science to help analyse increasing volumes of data (Bergen et al., 2019).

Fortunately, the engineering geology community has largely embraced digital geoscience. Consequently, the concept of the 3D engineering geological model and its function in storing and understanding the spatial distribution of subsurface discontinuities, engineering properties and their changes over time is one that has evolved alongside technological developments in recent years (Culshaw, 2005, Fookes, 1997). Geophysical investigation has always played a niche but important role in ground investigation. It is interesting to note that the Engineering Geology Unit of the British Geological Survey (BGS), first started in the 1960s, included the use of geophysics as a core part of its activities from its creation (for a history of engineering geology within the BGS, see the summary by Culshaw et al., 2019), and was an early adopter of the term 'engineering geophysics' within the context of UK engineering geology practice (Hooper, 1983).

However, despite geophysics embracing and benefitting from many of leaps in digital technologies in recent decades (e.g., hardware miniaturisation, better battery and data storage, wireless telecommunications, increased computing power and affordability, open-source software development), the way in which geophysics is applied to site investigation has changed little in recent decades, typically either being employed to screen

sites prior to intrusive investigation, or to delineate unexpected features arising during intrusive works that might prove problematic or hazardous to further ground investigation. In the experience of the authors, geophysical survey deliverables still typically comprise 2D graphical representations of data rather than digital models that can be visualised and analysed in a 3D environment. More widely, the challenges faced by geophysicists operating in the ground engineering sphere as summarised by Annan (1997) over two decades ago, could still apply in some cases today. These challenges include: understanding the requirements of engineers and communicating geophysical results in an understandable format, quantifying cost benefits, and maintaining professional standards of practice.

In this paper, we highlight three major developments that stand to improve the usefulness and integration of geophysical investigations within ground engineering, particularly within the context of ground investigation for hazard identification. These developments include: i) the maturation of 3D geophysical imaging techniques to solve 3D geotechnical problems, ii) better integration of data using multi-method geophysical surveys and / or field-estimated or laboratory-measured geotechnical properties and relationships, and iii) improved data inversion, integration, interpretation and visualisation using open-source, community-supported software packages. We suggest these points as key areas as they align with trends in how 3D digital datasets for ground modelling (outside of geophysics) are obtained, analysed and visualised.

To demonstrate these developments in practice, we present the results of a 3D electrical resistivity tomography (ERT) survey used to investigate the ground for areas of variable lithology and strength, including the presence of potential sinkholes and karst features, in the East Midlands, England. ERT has been used in many previous studies to delineate subsurface karstic features (see examples by Cheng et al., 2019, Nyquist et al., 2007, Zhu et al., 2011). Although using 3D ERT is not a novel approach to mapping subsurface karstic features, its use beyond academic studies as part of a commercial ground investigation is still relatively uncommon. Hence, in addition to demonstrating the technical benefits of 3D ERT, we highlight the novel and integrated phased approach to both the intrusive and geophysical investigations of the site.

2. Methods and materials

2.1 Electrical resistivity tomography

In a typical ERT survey, tens of electrodes are placed at shallow depths (10 – 20 cm) in a linear array along the ground surface. A resistivity meter connected to the electrode array via multi-core cables collects a pseudo-section of apparent resistivity measurements. Measurements are made by injecting DC current across a pair of (current) electrodes, and the potential is measured over a second pair of (potential) electrodes. From this, the bulk apparent resistivity of the ground at a point relative to the geometry of the surface electrodes is measured (Loke et al., 2013).

Depth of the apparent resistivity measurement is proportional to the spacing between the electrodes used for the measurement, with lateral position controlled by which electrodes are used along the profile. The depth of the shallowest and deepest reading is governed by the minimum spacing between electrodes and total number of electrodes used respectively. Hence, there is a trade-off between resolution and depth of investigation that needs to be balanced for the survey aims. In any case, there will always be a decrease in resolution with depth relative to near-surface measurements, which is a consideration in all geophysical methods. A measurement of resistivity is influenced by several factors in the ground, primarily the presence and conductivity of pore fluids (the presence of which will reduce resistivity), lithology (resistivity of rocks and soils varies over 20 orders of magnitude), the clay-content of the material (the presence of clay reduces resistivity) and the porosity of the medium (with increased porosity tending to increase resistivity if pores are air-filled).

Field ERT data are inverted to produce modelled cross-sections of resistivity. Inversion can broadly be regarded as the opposite of forward modelling. In a forward model, the model is known, and data are predicted (e.g., calculating the magnetic field lines of a bar magnet with known dimensions and magnetic strength). The opposite is true for an ERT survey; the data (e.g., the magnetic field lines) are known, but the model (the dimensions and strength of the bar magnet) is not, and so data inversion iteratively minimises (through repeated inversion and forward modelling) the misfit between observed data and a modelled solution. Different models can produce the same data, a concept known as ‘non-uniqueness’ (e.g., a large, weakly magnetic bar magnet can produce a similar magnetic field to a small, strongly magnetic bar magnet). It is therefore pertinent to keep in mind that the outputs of geophysical inversion are modelled solutions and not direct measurements of the ground conditions; the map is not the territory.

Where there are localised variations in ground conditions adjacent to an ERT profile, the injected current can be distorted by these off-line features (particularly where conductive features are present, through which current might preferentially flow). These off-profile distortions can create data artefacts in 2D models and are commonly referred to as '3D effects' (Dahlin et al., 2007). Data artefacts from 3D effects can be mitigated by using multiple 2D profiles to acquire parallel profiles of data at regular intervals and then inverting the data from all profiles using a 3D inversion algorithm, as opposed to inverting individual profiles using a 2D algorithm (Dahlin and Loke, 1997). The specification for a successful 3D survey is more intensive than a 2D survey due to the higher density of data coverage required, and the inversion of data is far more computationally expensive. However, the result of this process is a single 3D volume of data. In heterogenous environments, this approach can provide far more insight in to ground conditions than by using sparsely separated 2D profiles, which i) may also suffer from 3D effects not accounted for in the inversion process, and ii) may still not capture small-scale heterogeneity in ground conditions in the spaces between individual profiles.

3. Welby Overflow site investigation

3.1 Project rationale and site description

The Welby Overflow (WO) site comprises the northern parts of two arable fields (eastern and western fields) located approximately 6.6 km east of Grantham and 1.3 km south of the village of Welby in Lincolnshire, England (Figure 1). The site is being developed as part of Anglian Water's Strategic Pipeline Alliance (SPA), which will construct hundreds of kilometres of interconnected water mains across the east of England to build resilience across the network. A tank, lagoon and pumping station are planned for constructed at the WO site.

A potential risk to this development is the presence of karst and eroded surfaces at the upper boundary of the Upper Lincolnshire Limestone Member (ULLM). The ULLM is described as an ooidal and shell fragmented grainstone. Superficial deposits comprising mid-Pleistocene glaciofluvial deposits of sands and gravels are mapped across parts of the site, which may infill topographic incisions and depressions of the upper surface of the ULLM. This presents several risks including differential settlement, channelised drainage of subsurface water and associated washout (Waltham and Fookes, 2003). Mapping the scale and location of these features allows for risks to be minimised in design, enhancing long-term resilience of the planned structures.

A historic borehole (BGS Reference: SK93NE18) is located in the north eastern corner of the eastern field. This borehole indicates a 0.76 m thick cover of superficial deposits overlying ooilitic limestone extending to 24.72 m bgl. A 0.3 m band of clay is identified at the base of this oolitic limestone and is underlain by limestone to a depth of ~28 m bgl, at which point a transition zone of sandy clay and ironstone is identified above the blue clays of the Upper Lias Formation at ~29 m bgl.

3.2 Initial geophysical and ground investigation

To identify areas of superficial deposits and strength variations in the ULLM, SPA commissioned a geophysical survey of parts of the eastern and western fields at the WO site. This survey was undertaken by TerraDat in December 2021 and March 2022 (the second phase of geophysics taking place after initial intrusive ground investigation, which was undertaken in February 2022). The initial geophysical survey used electromagnetic (EM) surveying and 2D ERT profiles to map the glaciofluvial deposits at the WO site. The EM survey mapped the lateral extents of the glaciofluvial deposits (which are markedly more conductive than the ULLM due to their increased clay content), and several ERT profiles indicated variations in the 2D resistivity profile of the ULLM interpreted as potential clay-rich infill material. Furthermore, deeper conductive features in the ERT profiles were interpreted as geological boundaries, potential solution features or fracture zones.

The initial phase of ground investigation confirmed the variable thickness of glaciofluvial sands, clays and gravels across the WO site. The western field was shown to have significantly increased thicknesses of glaciofluvial deposits in areas corresponding to increased conductivity in the EM survey and decreased resistivity (the inverse measurement of conductivity) in the ERT sections. For this reason, the locations of the proposed tanks were moved to the eastern field. However, the TerraDat EM survey was not specified to completely cover the eastern section of this field and the ERT profiles provided only sparse coverage in the east. Furthermore, BGS mapping indicates further glaciofluvial deposits in the eastern part of the field. Hence, SPA commissioned a follow-up geophysical survey by Atkins to extend the footprint of the original survey undertaken by TerraDat, and to provide high-resolution 3D data to identify variability of the ULLM and thickness of overlying glaciofluvial materials.

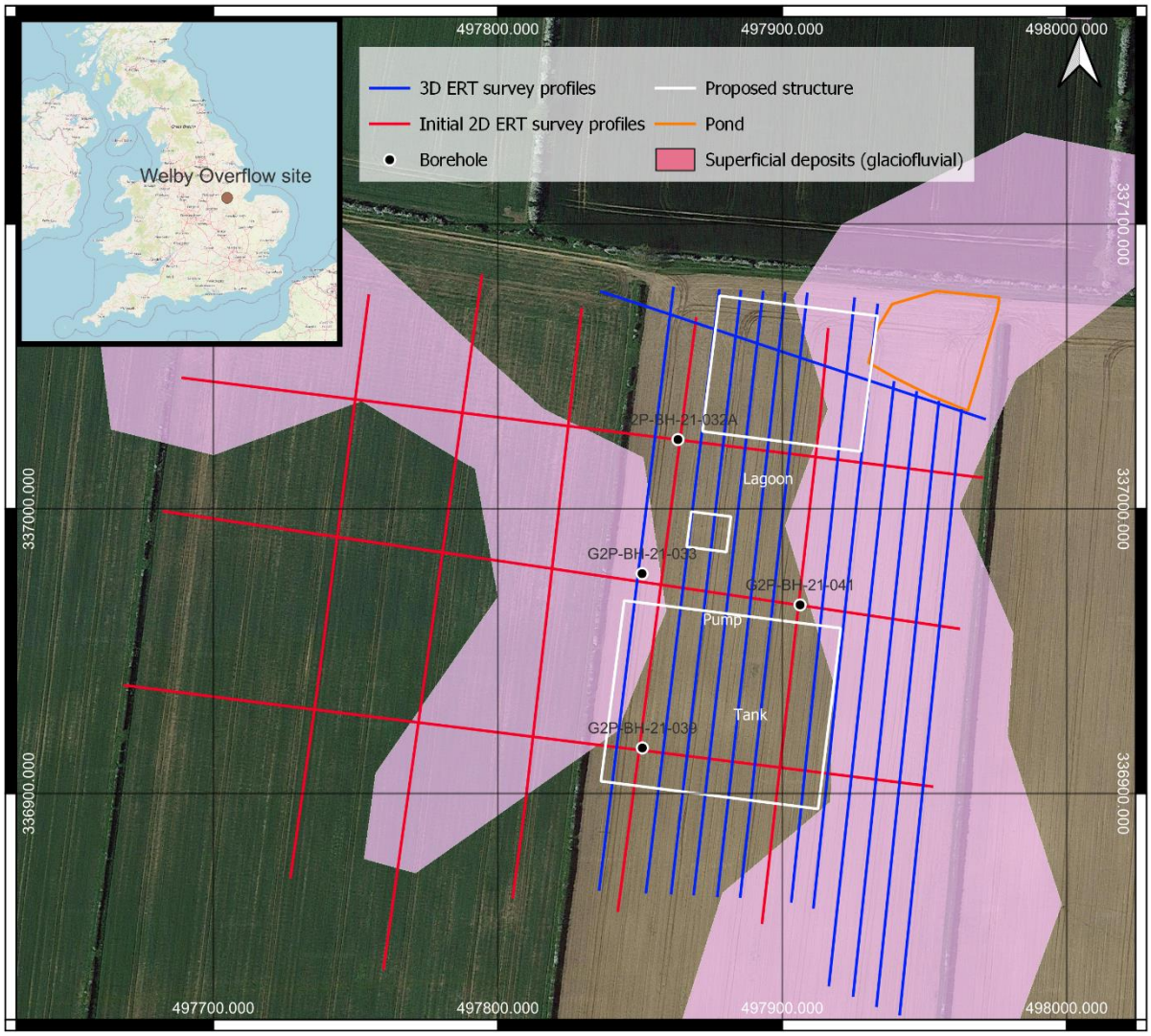

Figure 1: Map of the Welby Overflow site.

3.3 3D ERT survey acquisition

Atkins designed the 3D survey to incorporate previous profiles acquired by TerraDat, reducing the need for acquiring additional data on site by ~15%. We acquired 13 additional ERT profiles at regular intervals (~8 m apart) situated between the existing north – south orientated TerraDat profiles (located ~50 m apart). The data acquisition files for the Syscal Pro resistivity meter were designed to the same specification as the TerraDat surveys, using a Wenner-Schlumberger configuration set to investigate up to 20 m bgl. The survey was completed in November 2022, and to complete the survey in four days, electrodes were deployed at 3 m spacing (the TerraDat survey used 2 m spacing). A pond located in the north eastern corner of the field was identified during the pre-survey walkover, and the four eastern profiles had to be moved south to accommodate this feature. Field quality control and assessment showed the data quality to be high, with all individual model 2D inversions converging with root-mean square (RMS) errors of less than 5% after three inversion iterations.

We processed the 15 ERT profiles (2 profiles form the TerraDat survey and 13 from the Atkins survey) using two inversion algorithms; firstly using the open-source, Python-based ERT inversion software ResIPy (Blanchy et al., 2020), and secondly the licensed inversion software Res3DInv (Loke and Barker, 1996). Both inversions used an estimated error model, as field error data from reciprocal measurements were unavailable. Nevertheless, the ResIPy model converged after three inversions with an RMS error of ~1% and the Res3DInv model converged with an RMS error of 1.82% after 7 iterations. Both models showed good agreement on the 3D distributions of resistivity values across the area surveyed. Due to the spacing between profiles being slightly larger than optimal (profile spacings should typically approximately double the electrode spacing), some data artefacts are present in the near-surface (top 2 m) of both models, which present as linear extents of marginally lower resistivity

between the surveyed profiles. However, these artefacts are minor and are not present at the depths under investigation. The results of the Res3DInv model are presented in this study, as the model provides better resolution at depth and smoother resistivity distributions. However, the ResIPy model would still lead to the same conclusions being drawn in the following analysis.

4. Results and discussion

4.1 3D ERT survey results

We trimmed the extents of the 3D block to remove areas of poor coverage due to profile displacements (except the north eastern corner where the pond was located, which is disregarded in the model analysis). The model resistivity ranges from 20 – 1,000 Ω.m, with deeper parts of the model showing higher resistivity values (Figure 2). The hypothesis for interpreting the data is that stronger limestone should present as area of increased resistivity, as dissolution, fracturing (especially where fractures show clay infill) and increased saturation (which should lower bulk resistivity) will weaken the ULLM rock mass and reduce resistivity.

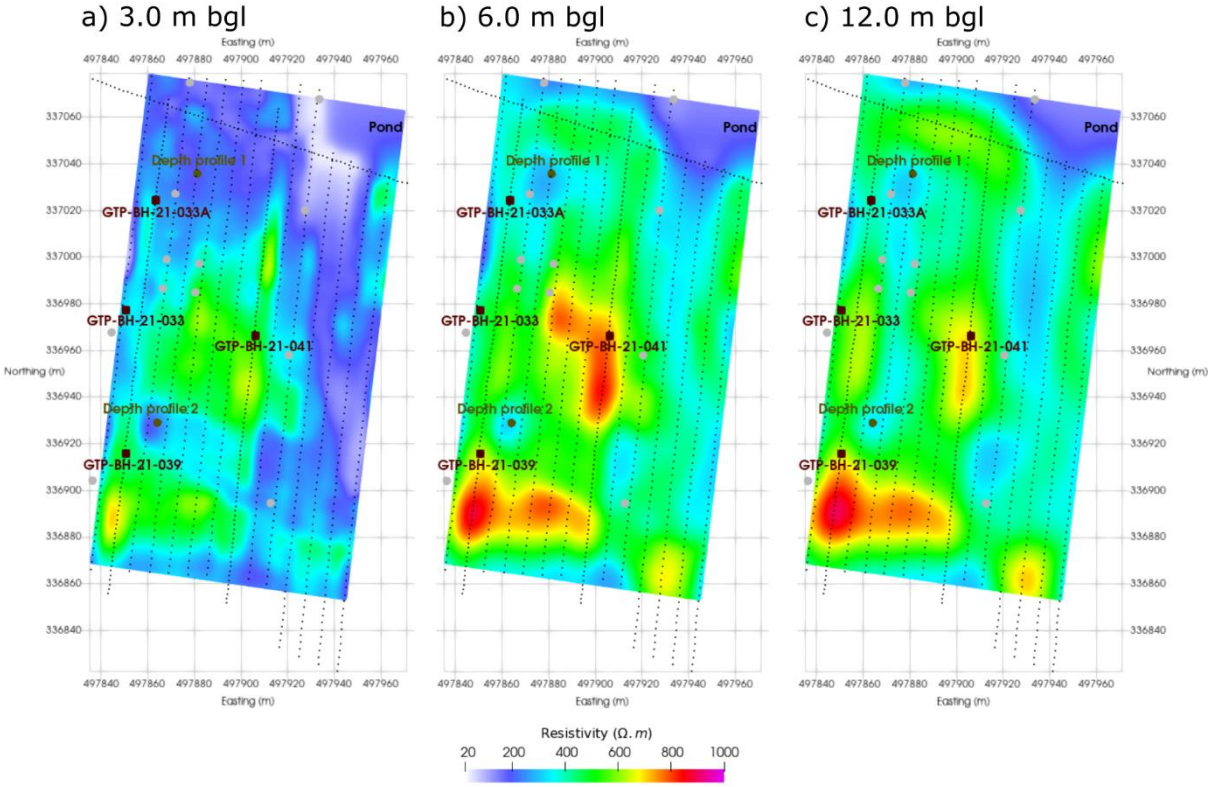

Figure 2: Depth slices at a) 3 m, b) 6 m and c) 12 m bgl through the 3D electrical resistivity tomography model. Electrode positions indicated by black dots.

We interpret the area of low resistivity (~20 Ω.m) in the north eastern corner (Figure 2a) as shallow seepage of surface water from the surface pond. At 6 m and 12 m bgl (Figures 2b and 2c respectively), north – south trending zones of lower resistivity are observed, interspersed with zones of higher resistivity values. We interpret these features as areas of glacial scouring, potentially infilled by glaciofluvial sediments. The widest of these features, to the east of the survey area, corresponds to a mapped deposit of glaciofluvial deposits (Figure 1), and the resistivity of this features may be reduced by seepage of surface water from the pond at the surface.

4.2 Integration of geophysical results with borehole data

The four boreholes drilled within the area of the 3D ERT survey identify the upper boundary of the ULLM between 1.7 and 2.8 m bgl. The engineering logs described the ULLM in three states: weak, medium and strong. Fractures are identified across all logs, with fracture indices ranging from 2 to 18. To identify zones of potential weaker ULLM, or zones of infill with glaciofluvial material, we extract the modelled resistivity values from each borehole location for depths at which limestone is recorded (Figure 3). From the four resistivity depth profiles, we indicate where weak, medium and strong limestones are recorded. Although there is significant variability in

the resistivity of strong limestones (~350 - ~720 Ω.m) and medium limestone (~380 - ~720 Ω.m), all recorded instances of weak limestone show resistivity values of less than 400 Ω.m. A key assumption is that there is statistical correlation between the one borehole showing both weak limestone and low resistivity, and that this correlation can be extended across the entire model. However, previous studies show that karstic features tend to manifest as areas of lower resistivity (e.g., Nyquist et al., 2007). It is worth noting that large volumes of the 3D ERT model show resistivity values <400 Ω.m (Figure 2), although this should not be taken as a definitive threshold at which weaker limestones are present.

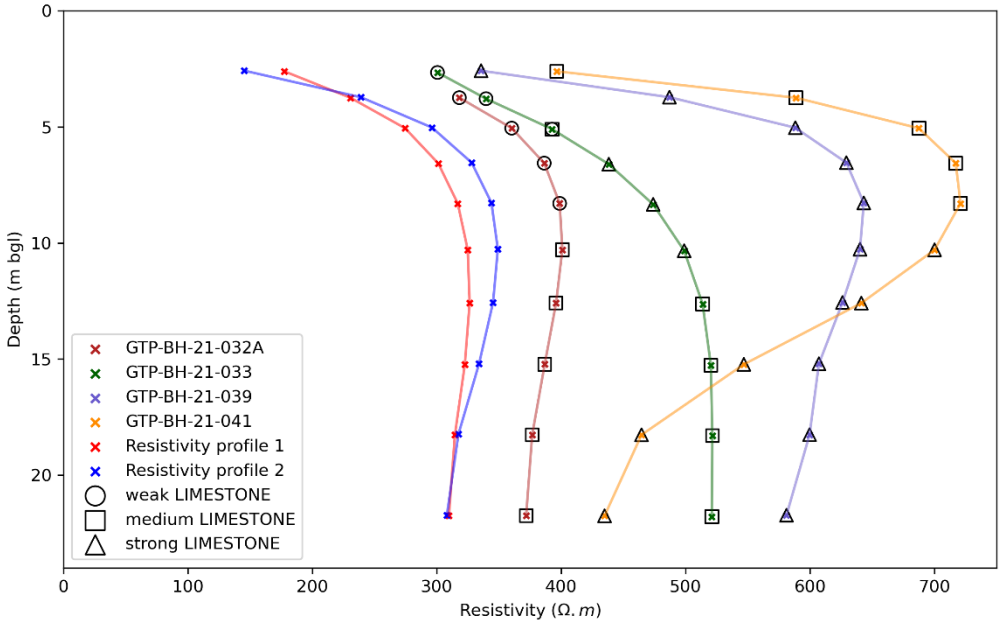

Figure 3: Resistivity-depth profiles from the four boreholes drilled within the 3D ERT survey area, and two locations of low resistivity within the bounds of proposed structures. Strength of limestone from engineering logs of the borehole resistivity-depth profiles.

Although a direct relationship between resistivity and strength of the ULLM is unlikely to exist, we extract two resistivity profiles from the 3D models, to investigate the resistivity-depth relationship of two low resistivity zones within the footprint of the lagoon and tank structures (see 'Depth profiles' locations, Figure 2). These locations both show resistivity values lower than those points recorded as weak limestone in the boreholes, suggesting the presence of weak limestone and / or increased clay content in these zones. Hence, these areas have been marked for follow up drilling to investigate the cause of these low resistivities.

5. Conclusions

This study highlights that the product of a 3D geophysical survey is a multi-dimensional, high-resolution digital model that provides extensive insight into the distribution of engineering properties. The heterogeneity of some environments, such as karst settings, can vary significantly across small distances, and can be difficult to capture using intrusive methods alone. In this study, three of the four boreholes encountered strong ULLM. However, the ERT survey suggests that the proportion of strong limestone may be much lower across the site, and large volumes of the 3D model showing resistivity values lower than that of intact limestone. At the time of writing, further boreholes are being planned to investigate the low-resistivity features identified in the 3D ERT model. It will be interesting to integrate this data further into the analysis undertaken in this paper and explore the use of automatic classification techniques to identify geophysical-geotechnical relationships (e.g., Whiteley et al., 2021).

Geophysical surveys, particularly when undertaken in 3D, are uniquely placed to fill an important knowledge gap that sits between the high-resolution, but surface-only, observations gleaned from remote sensing, and the detailed but extremely localised data from intrusive ground investigation. In this sense, geophysical surveys can be considered a vital source of information with which to supplement 3D model development, particularly in the context of identifying geohazards associated with heterogeneous ground conditions.

Acknowledgements

The authors present with the permission of SPA and acknowledge V. Tibra, M. Edmondson, L. Henriques, I. Griffiths and C. Tan for their input, and especially thank Chloe Rushworth (Atkins) for her efforts in the field.

References

Annan, A. P. (1997). Engineering and environmental geophysics: the future. 12**,** 419-426.

Bergen, K. J., Johnson, P. A., De Hoop, M. V. & Beroza, G. C. (2019). Machine learning for data-driven discovery in solid Earth geoscience. *Science*, 363**,** 0323.

Blanchy, G., Saneiyan, S., Boyd, J., McLachlan, P. and Binley, A. (2020). ResIPy, an Intuitive Open Source Software for Complex Geoelectrical Inversion/Modeling. *Computers & Geosciences*, February, 104423. https://doi.org/10.1016/j.cageo.2020.104423.

Cheng, Q., Chen, X., Tao, M. & Binley, A. (2019). Characterization of karst structures using quasi-3D electrical resistivity tomography. *Environmental Earth Sciences,* 78**,** 285.

Culshaw, M. G. (2005). From concept towards reality: developing the attributed 3D geological model of the shallow subsurface. *Quarterly Journal of Engineering Geology and Hydrogeology,* 38**,** 231-284.

Culshaw, M. G., Northmore, K. J. & Mccann, D. M. (2019). A Short History of Engineering Geology and Geophysics at the British Geological Survey—Part 2: Engineering Geological Mapping. Cham. Springer International Publishing, 45-52.

Dahlin, T. & H. Loke, M. (1997). Quasi-3D resistivity imaging - mapping of three dimensional structures using two dimensional DC resistivity techniques.

Dahlin, T., Wisén, R. & Zhang, D. (2007). 3D Effects on 2D Resistivity Imaging – Modelling and Field Surveying Results.

Fookes, P. G. (1997). Geology for Engineers: the Geological Model, Prediction and Performance. *Quarterly Journal of Engineering Geology and Hydrogeology,* 30**,** 293-424.

Griffiths, J. S. (2019). Advances in engineering geology in the UK 1950–2018. *Quarterly Journal of Engineering Geology and Hydrogeology,* 52**,** 401-413.

Hearn, G. J. (2019). Discussion on 'Advances in engineering geology in the UK 1950–2018', *Quarterly Journal of Engineering Geology and Hydrogeology,* 52**,** 563-568.

Hooper, J. W. (1983). Engineering geophysics. *Quarterly Journal of Engineering Geology and Hydrogeology,* 16**,** 247-249.

Loke, M. H. & Barker, R. D. (1996). Rapid least-squares inversion of apparent resistivity pseudosections by a quasi-Newton method 1. *Geophysical prospecting,* 44**,** 131-152.

Loke, M. H., Chambers, J. E., Rucker, D. F., Kuras, O. & Wilkinson, P. B. (2013). Recent developments in the direct-current geoelectrical imaging method. *Journal of Applied Geophysics,* 95**,** 135-156.

Mccaffrey, K. J. W., Jones, R. R., Holdsworth, R. E., Wilson, R. W., Clegg, P., Imber, J., Holliman, N. & Trinks, I. (2005). Unlocking the spatial dimension: digital technologies and the future of geoscience fieldwork. *Journal of the Geological Society,* 162**,** 927-938.

Nyquist, J. E., Peake, J. S. & Roth, M. J. S. (2007). Comparison of an optimized resistivity array with dipole-dipole soundings in karst terrain. *GEOPHYSICS,* 72**,** F139-F144.

Waltham, A. C. & Fookes, P. G. (2003). Engineering classification of karst ground conditions. *Quarterly Journal of Engineering Geology and Hydrogeology,* 36**,** 101-118.

Whiteley, J., Watlet, A., Uhlemann, S., Wilkinson, P., Boyd, J. P., Jordan, C., Kendall, J. M. & Chambers, J. E. (2021). Rapid characterisation of landslide heterogeneity using unsupervised classification of electrical resistivity and seismic refraction surveys. *Engineering Geology*, 290, 106189.

Zhu, J., Currens, J. C. & Dinger, J. S. (2011). Challenges of using electrical resistivity method to locate karst conduits—A field case in the Inner Bluegrass Region, Kentucky. *Journal of Applied Geophysics,* 75**,** 523-530.

INTERNATIONAL SOCIETY FOR SOIL MECHANICS AND GEOTECHNICAL ENGINEERING

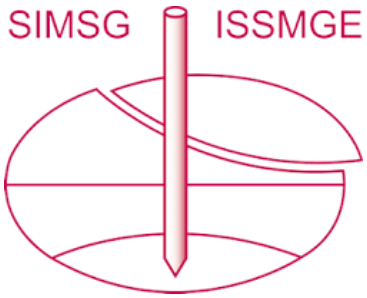

This paper was downloaded from the Online Library of the International Society for Soil Mechanics and Geotechnical Engineering (ISSMGE). The library is available here:

https://www.issmge.org/publications/online-library

This is an open-access database that archives thousands of papers published under the Auspices of the ISSMGE and maintained by the Innovation and Development Committee of ISSMGE.

The paper was published in the proceedings of the Geo-Resilience 2023 conference which was organized by the British Geotechnical Association and edited by David Toll and Mike Winter. The conference was held in Cardiff, Wales on 28-29 March 2023.